Received: 4 July 2023 | Revised: 30 April 2024 | Accepted: 7 May 2024

DOI: 10.1096/fj.202301325R

RESEARCH ARTICLE

The FASEB Journal

The endocannabinoid anandamide activates pro-resolving pathways in human primary macrophages by engaging both CB_2 and GPR18 receptors

Alessandro Leuti[1,2] | Marina Fava[1,2] | Giulia Forte[1] | Niccolò Pellegrini[1] | Sergio Oddi[2,3] | Lucia Scipioni[2,4] | Esteban A. Gomez[5] | Jesmond Dalli[5,6] | Mauro Maccarrone[2,4]

[1]Department of Medicine, Campus Bio-Medico University of Rome, Rome, Italy

[2]European Center for Brain Research/ Institute for Research and Health Care (IRCCS) Santa Lucia Foundation, Rome, Italy

[3]Department of Veterinary Medicine, University of Teramo, Teramo, Italy

[4]Department of Biotechnological and Applied Clinical Sciences, University of L'Aquila, L'Aquila, Italy

[5]Centre for Inflammation and Therapeutic Innovation, Queen Mary University of London, London, UK

[6]William Harvey Research Institute, Queen Mary University of London, London, UK

Correspondence
Alessandro Leuti, Department of Medicine, Campus Bio-Medico University of Rome, Rome, Italy.
Email: a.leuti@unicampus.it

Mauro Maccarrone, Department of Biotechnological and Applied Clinical Sciences, University of L'Aquila, L'Aquila, Italy.
Email: mauro.maccarrone@univaq.it

Funding information
Ministero della Salute, Grant/Award Number: PNRR-MAD-2022-12376730

Abstract

Resolution of inflammation is the cellular and molecular process that protects from widespread and uncontrolled inflammation and restores tissue function in the aftermath of acute immune events. This process is orchestrated by specialized pro-resolving mediators (SPM), a class of bioactive lipids able to reduce immune activation and promote removal of tissue debris and apoptotic cells by macrophages. Although SPMs are the lipid class that has been best studied for its role in facilitating the resolution of self-limited inflammation, a number of other lipid signals, including endocannabinoids, also exert protective immunomodulatory effects on immune cells, including macrophages. These observations suggest that endocannabinoids may also display pro-resolving actions. Interestingly, the endocannabinoid anandamide (AEA) is not only known to bind canonical type 1 and type 2 cannabinoid receptors (CB_1 and CB_2) but also to engage SPM-binding receptors such as GPR18. This suggests that AEA may also contribute to the governing of resolution processes. In order to interrogate this hypothesis, we investigated the ability of AEA to induce pro-resolving responses by classically-activated primary human monocyte-derived macrophages (MoDM). We found that AEA, at nanomolar concentration, enhances efferocytosis in MoDMs in a CB_2- and GPR18-dependent manner. Using lipid mediator profiling, we also observed that AEA modulates SPM profiles in these cells, including levels of resolvin (Rv)D1, RvD6, maresin (MaR)2, and RvE1 in a CB_2-dependent manner. AEA treatment also modulated the gene expression of SPM enzymes involved in both the formation and further metabolism of SPM such as 5-lipoxygenase and 15-Prostaglandin dehydrogenase. Our findings show, for the first time, a direct effect of AEA on the regulation of pro-resolving pathways in human macrophages. They also provide

Alessandro Leuti and Marina Fava contributed equally to this work.

Jesmond Dalli and Mauro Maccarrone contributed equally to this work.

new insights into the complex interactions between different lipid pathways in activation of pro-resolving responses contributing to the reestablishment of homeostasis in the aftermath of acute inflammation.

1 | INTRODUCTION

Resolution of inflammation is the cellular and molecular process that acts as a fail-safe on immune events to avoid uncontrolled acute inflammation that would lead to chronic phlogosis and impairment of tissue function.[1] This pivotal homeostatic process is determined by the production and activity of a host of arachidonic (AA)-, docosahexaenoic (DHA)-, docosapentaenoic (DPA)- and eicosapentaenoic (EPA)-derived bioactive lipids, altogether termed specialized pro-resolving mediators (SPM), which include D- and E-series resolvins (RvDs and RvEs, respectively), maresins (MaRs), protectins, and lipoxins (LXs).[1] These bioactive lipids are mostly produced by monocytes/macrophages, polymorphonuclear cells, and hypoxic endothelia during acute inflammation through the activity of 5-/12-/15-lipoxygenase (ALOX5, ALOX12, and ALOX15) and cyclooxygenase 2 (COX2)/cytochrome P450 (CYP450)-dependent pathways.[2]

SPMs include more than 40 lipid mediators that act in concert to hinder the influx of immune cells at the inflamed site, induce phagocytic clearance of apoptotic cells (i.e., efferocytosis), and oppose to the pro-inflammatory activation of macrophages and lymphocytes.[1,3,4] Studies conducted in the past two decades identified other lipid signals that partake in the initiation and outcome of the immune event. The production of these molecules was also observed to be dysfunctional during the derangement of the inflammatory processes,[5,6] thus suggesting that other non-SPMs lipid mediators might participate in the resolution network. Among these lipid moieties, endocannabinoids (eCBs) – i.e., the endogenous ligands to the type 1 and type 2 cannabinoid receptors (CB_1 and CB_2), which also bind the psychoactive compound of *Cannabis sativa* Δ^9-tetrahydrocannabinol – represent prominent examples. The eCBs modulate several cellular components of the immune system, including those of the innate branch.[5,6] These molecules include *N*-arachidonoylethanolamine (AEA or anandamide) and 2-arachidonoylglycerol (2-AG), the former being able to reduce the release of pro-inflammatory cytokines in both T lymphocytes and monocyte/macrophages in a CB_2-dependent manner.[5,7,8] Interestingly, only a handful of SPM receptors have been characterized to date, most of them in the past decade.[9] Some of these receptors exhibit eCB-binding properties: indeed, GPR18 is activated by both RvD2[10] and AEA.[11] Of note, CB_2 agonism enhances efferocytosis – one of the key processes during resolution of inflammation – in mouse-derived macrophage cell lines and primary cultures.[12] This evidence strongly advocates for a role for eCBs – especially AEA – as adjuvants in the resolution program, which might enhance resolution in macrophages not only by potentiating their phagocytic activities but also by enhancing SPMs biosynthesis during inflammatory conditions. Yet, the role of AEA in activating resolution processes, particularly in the context of macrophage-dependent processes, has been poorly investigated to date. In this perspective, macrophages are primary orchestrators of the immune response and of the resolution program, which promote resolution and tissue regeneration through efferocytosis; in addition, they produce SPMs and are target of their activity.[3] Thus, the modulation of their pro-resolving/immunomodulatory properties by means of a synergy between the SPMs and eCBs appears relevant to understand the full extent of the mechanisms that partake in tissue homeostasis.

Against this background, in the present work we ascertained the ability of AEA – which is the only known eCB able to engage an SPM-binding receptor such as GPR18 – to induce bona fide pro-resolving effects in primary human monocyte-derived macrophages (MoDMs), in order to interrogate whether this eCB can be involved in the resolution program.

2 | MATERIALS AND METHODS

2.1 | Peripheral blood cell isolation and macrophage differentiation and treatment

Peripheral blood mononuclear cells (PBMCs) were isolated from whole blood diluted with PBS in a 1:1 (vol/vol) ratio and were separated by density gradient centrifugation over Histopaque-1077. The ring containing the PBMCs at the interphase between Histopaque and plasma was collected in a new sterile tube and washed twice with PBS at 1500 rpm for 10 min with maximum acceleration and brakes at RT. PBMCs were then resuspendend in Ca^{2+}/Mg^{2+} PBS and were allowed to adhere for 45 min at 37°C. Adherent cells were then washed with Ca^{2+}/Mg^{2+}–free PBS and incubated at 37°C and 5% CO_2 in RPMI-1640 medium (Sigma) containing 1% Penicillin/Streptomycin solution (Sigma), 25 ng/mL macrophage colony-stimulating factor (M-CSF, Miltenyi) and AEA 50 nM-2.5 μM or ethanol

0.01% as vehicle. After 1 h, the culture medium was supplemented with 10% human serum (male A/B; Sigma). Cells were rinsed every 2 days, and culture medium, with AEA/vehicle and M-CSF was added. On day 8, cells were rinsed and incubated in complete RPMI-1640 supplemented with 100 ng/mL LPS and 10 ng/mL IFNγ for 2 days. Cells and their supernatants were harvested and used for the following cellular and molecular analyses.

2.2 | Efferocytosis assay

Classically activated MoDMs were seeded in 96-well plates at 5×10^4 cells/well. Efferocytosis assays were performed as reported in Flak et al.[13]; in brief: Apoptotic target cells were generated as follows: human promyelocytic HL-60 cells were seeded at 1×10^6 cells/mL onto 35-mm plates, irradiated with UV-C light (254 nm) for 15 min, followed by incubation at 37°C and 5% CO_2 for 2 h. Induction of apoptosis was confirmed by flow cytometry using the APC Annexin V Apoptosis Detection Kit with PI (BioLegend), with Annexin V-positive and Annexin V/PI-double positive cells considered to be apoptotic.

Apoptotic HL-60 cells were washed with PBS and labeled with 1 μM pHrodo Red Succinimidyl Ester (Invitrogen, Thermo Fisher Scientific) in PBS for 30 min at room temperature. Classically activated MoDMs were stained with CellBrite® Green (Biotium) for 1 hour at 37°C to visualize cell membranes, washed with serum-free RPMI-1640 medium (Invitrogen), and incubated with AEA (50 nM–2.5 μM) or 2-AG (100 nM–1 uM) or URB-597 (5uM) or vehicle (RPMI-1640 containing 0.01% ethanol) for 45 min at 37°C and 5% CO_2. Then, pHrodo Red-labeled HL-60 was added directly to the macrophages at a 3:1 ratio (apoptotic HL-60/macrophage) and the increase in pHrodo fluorescent signal over time was quantified using a Zeiss Cell discoverer 7 high-content imager (Zeiss) system set up with appropriate filters and incubation at 37°C and 5% CO_2. Efferocytosis was determined by dividing pHrodo fluorescent signal by CellBrite® Green-stained cell counts for each time point and by calculating the fluorescence at 50 and 120 min from the beginning of the exposition to apoptotic HL-60 cells or the area under the curve.

2.3 | Gene siRNA-mediated silencing of GPR18 and CB_2 in monocyte-derived macrophages

PBMCs isolated using Ficoll paque PLUS density centrifugation from blood cones were plated onto 10-cm tissue culture plates and incubated at 37°C for 1 hour in Ca^{2+}/Mg^{2+}PBS. Subsequently, cells were washed using PBS and adherent cells were incubated in RPMI 1640 containing 10% human serum and 25 ng/mL macrophage-colony-stimulating factor (M-CSF) for 6 days at 37°C in 5% CO_2. On day 6, monocyte-derived macrophages were then seeded onto 96-well plates at 5×10^4 cells per well and transfected with 1 μM Accell Human Control siRNA or Accell Anti-human GPR18 siRNA SMARTpool or Anti-human CB_2 siRNA for 72 hours in serum-free Accell siRNA Delivery Medium (Dharmacon, Colorado, US). On day 9 cells were incubated with AEA (100, 500 nM) or URB (5uM) or 2-AG (100 nM–1 uM) or vehicle (RPMI-1640 containing 0.1% ethanol) for 48 h at 37°C. GPR18 and CB_2 expression was assessed through flow cytometry using anti−CB_2 (Abcam) and anti−GPR18 (Novus Bio) primary antibodies for 40 min at 4°C and Alexa Fluor 465-rabbit secondary antibody for 30 min.

2.4 | Quantitative real-time PCR

Total RNA was extracted with ReliaPrep RNA cell Mniprep System kit (Promega). A mixture containing random hexamers, oligo(dT)15 (Promega), and SuperScript II Reverse Transcriptase (Invitrogen) was used for cDNA synthesis. Transcripts were quantified by real-time quantitative PCR on an ABI PRISM 7900 sequence detector (Applied Biosystems) with Applied Biosystems predesigned TaqMan Gene Expression Assays and ABsolute QPCR ROX mix (Thermo Fisher Scientific). The following probes were used (Applied Biosystems, assay identification numbers in parentheses): GPR32 (Hs00265986_s1), GPR18 (Hs01921463_s1), ALX/FPR2 (Hs02759175_s1), ChemR23 (Hs01081979_s1), ALOX5 (Hs00167536_m1), ALOX12 (Hs00167524_m1), ALOX15 (Hs00993765_g1), 15-PGDH (Hs00960586_g1). Relative expression of each gene was normalized to the amount of beta-2 microglobulin (Hs00187542_m1).

2.5 | Liquid chromatography–tandem mass spectrometry (LC–MS/MS)

For lipid mediator analysis, cell lysates and supernatants were placed in two volumes of ice-cold methanol containing deuterated internal standards (d_4-LTB_4, d_4-PGE_2, d_5-MaR1, d_5-MaR2, d_5-RvD2, d_5-RvD3, d_5-RvE1, d_8-5S-HETE, d_5-LXA_4; Cayman Chemicals; Michigan, United States) representing each chromatographic region employed in the identification of the lipid mediator of interest. After the addition of methanol (Fisher Scientific), samples were placed at −20°C for a minimum of 45 min to facilitate protein precipitation. These were then centrifuged, and lipid mediators were extracted from the supernatants using an

ExtraHera System (Biotage, Uppsala, Sweden) and solid-phase methodologies with Isolute C18 500 mg columns (Biotage). Lipid mediators were eluted from the C18 columns using methyl formate (Sigma Aldrich). These were then brought to dryness and resuspended in methanol/Milli-Q water (1:1, vol/vol) for injection on a Shimadzu LC-20 AD HPLC and a Shimadzu SIL-20 AC autoinjector, paired with a QTrap 6500+ MS/MS (Sciex, Massachusetts, United States). In the analysis of mediators eluted in the methyl formate fraction, an Agilent Poroshell 120 EC-C18 column (100 mm × 4.6 mm × 2.7 μm) was kept at 50°C and mediators eluted using a mobile phase consisting of methanol/water/acetic acid of 20:80:0.01 (vol/vol/vol) that was ramped to 50:50:0.01 (vol/vol/vol) over 0.5 min and then to 80:20:0.01 (vol/vol/vol) from 2 min to 11 min, maintained till 14.5 min and then rapidly ramped to 98:2:0.01 (vol/vol/vol) for the next 0.1 min. This was subsequently maintained at 98:2:0.01 (vol/vol/vol) for 5.4 min, and the flow rate was maintained at 0.5 mL/min. The QTrap 6500+ was operated in negative ionization mode using a multiple reaction monitoring method as previously reported.[14] Each lipid mediator was identified using established criteria, including (i) matching retention time to synthetic or authentic standards, (ii)≥8 data points, and (iii) signal–to-noise ratio≥5. Calibration curves were obtained for each mediator using synthetic compound mixtures at 0.78, 1.56, 3.12, 6.25, 12.5, 25, 50, 100, and 200 pg that gave linear calibration curves with r^2 values of .98–.99. Where standard curves for specific molecules were unavailable, molecules with similar physical properties were used to calculate the concentrations as previously described.[14]

2.6 | Flow cytometry

For surface expression of SPM receptors, of macrophage immunophenotype and phagocytosis markers, cells were incubated with APC-conjugated anti-ChemR23 (1:50, Miltenyi Biotec), APC-Vio770-conjugated anti-CD206 (1:50, Miltenyi Biotec), PE-conjugated anti-CD80 (1:50, Miltenyi Biotec), PE-Vio770-conjugated anti-CD54 (1:50, Miltenyi Biotec), FITC-conjugated anti-CD163 (1:50, Miltenyi Biotec), PE-Cyanine7-conjugated anti-CD32 (1:50, eBioscience), APC-conjugated anti-CD36 (1:50, BioLegend) or with PE-conjugated anti-CD300f (1:50, BioLegend). For GPR32, incubation with primary anti-GPR32 (1:100, GeneTex) was followed by Alexa647-conjugated anti-rabbit secondary antibody. For intracellular staining of SPM-enzymes or MerTK, cells were fixed with 4% formaldehyde and incubated with conjugated anti-ALOX5 (1:50, Abcam) followed by goat anti-Rabbit Alexa647-conjugated secondary antibody (1:200, Invitrogen) or with PE-conjugated anti-15-PGDH (1:50, Novus Bio) in saponin 0.5%; Brilliant Violet421-conjugated-MerTK (1:50, BioLegend).

The expression of the aforementioned proteins was assayed by means of polychromatic flow cytometry in a Cytoflex analyzer (Beckman Coulter) and the samples were analyzed using Flow Logic analysis software (Inivai Technologies).

For each experiment, a minimum number of 10 000 events were analyzed.

2.7 | Confocal microscopy

Differentiated and stimulated macrophages were seeded on Chamberslides (Lab-Tek) at 1×10^5 cells/well and were fixed and stained with anti-CB_2 (1:500, R&D Systems), anti-GPR18 (1:500, Novus Bio), anti-PPARγ (1:500, Santa Cruz Biotechnology), or anti-TRPV1 (1:500, Santa Cruz Biotechnology) specific primary antibodies, before incubating the samples with Alexa 488-conjugated or Alexa 568-conjugated anti-mouse secondary antibodies (1:200, Invitrogen). Nuclei were visualized using Hoechst 33342 counterstaining. The expression of these receptors was visualized by confocal microscopy (Nikon Eclipse Ti2), performing image acquisition using NIS software (Nikon).

2.8 | Statistical analysis

All data are expressed as mean ± SEM. Differences between groups were evaluated by means of parametric (paired t-test) or non-parametric (Wilcoxon rank test) depending on the fact that normal distribution could be assumed – following Shapiro–Wilk test – for each experimental group. All statistical tests were performed using PRISM 9.0 (GraphPad Software) and p values <.05 were considered significant. Partial least square discriminant analysis (PLS-DA) and variable importance projection (VIP) score for multiparametric analysis were conducted using the Metaboanalyst as previously reported.[13,15] Pathway analysis was performed as reported in.[14]

3 | RESULTS

3.1 | AEA enhances efferocytosis in classically activated human primary monocyte-derived macrophages (MoDMs)

AEA induces immunomodulatory effects in immune cells,[7,8,16] macrophages,[17] and is known to bind to the RvD2 receptor GPR18.[11] However, the bona fide pro-resolving properties of this eCB in macrophages – which

are among the most important effectors during resolution – have been as yet poorly investigated.

In order to test the hypothesis that AEA plays a role in resolution by enhancing the immunomodulatory properties of macrophages, we measured the effect of a chronic treatment with AEA on the ability of human primary monocyte-derived macrophages (MoDM) to phagocytose apoptotic leukocytes – i.e., efferocytosis (Figure 1A). To this end, MoDMs were incubated with pHrodo-red labeled HL-60 cells that underwent UV-induced apoptosis, and phagocytosis was measured in the presence of increasing concentrations of AEA (50 nM, 100 nM, 500 nM, 1 μM, 2.5 μM, 5 μM) (Figure 1B) or 0.01% ethanol (Veh).

Exposure to apoptotic HL-60 cells resulted in increased pHrodo red in MoDMs, indicating efferocytosis of apoptotic bodies. AEA treatment resulted in a further enhancement in fluorescence, suggesting that the treatment with this eCB potentiated efferocytosis. In particular, MoDM

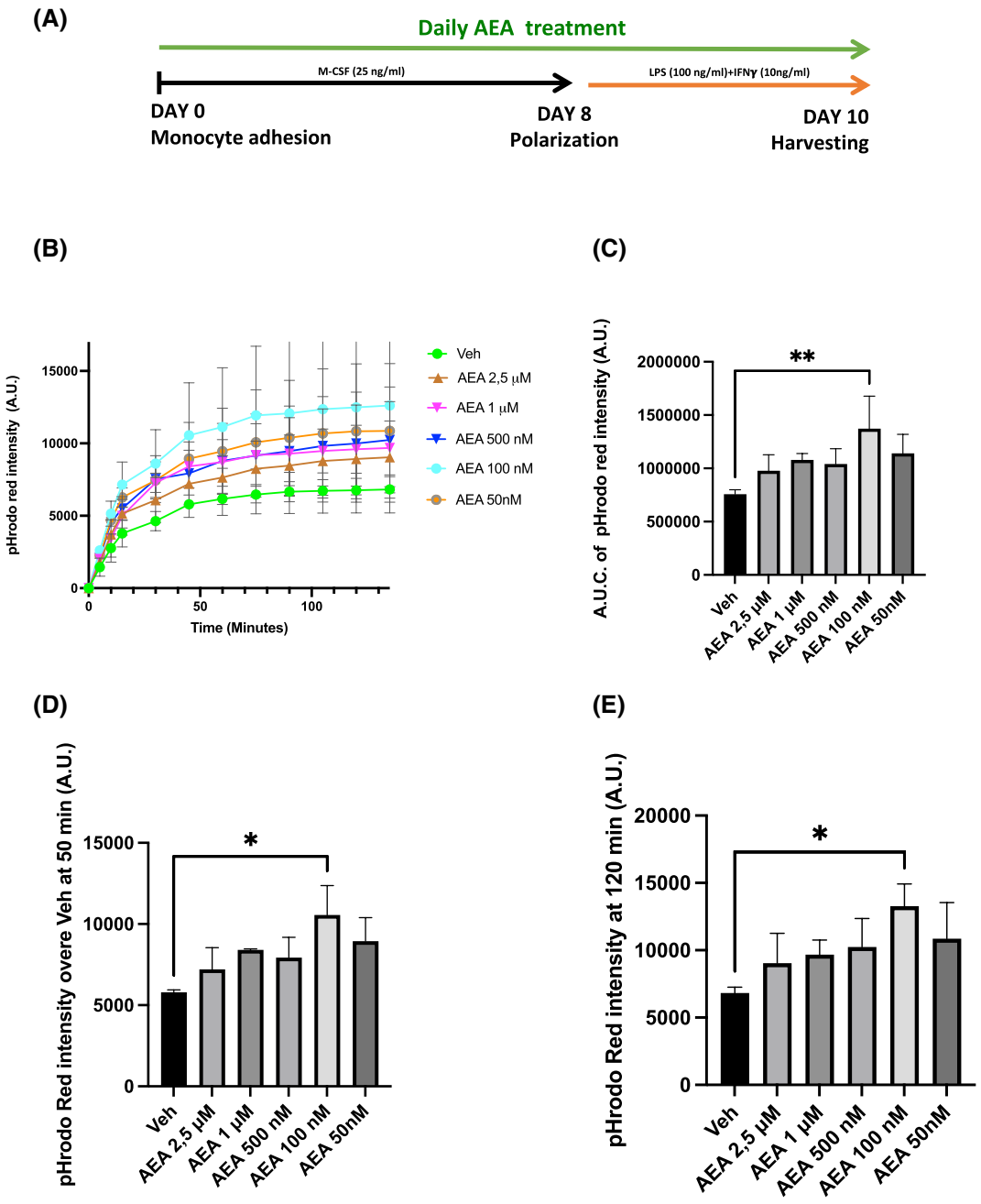

FIGURE 1 Dose-dependent effect of AEA on MoDM-dependent efferocytosis. Experimental setup used in the differentiation of PBMC-derived monocytes into MoDMs and their treatment with AEA(A). effect of AEA on the efferocytosis of pHrodo-labeled HL-60 apoptotic cells in AEA-treated MoDMs (B), with detail on the effect at 50 min (C) and 150 min (D) and on the area under the curve (A.U.C.) (E). Al data points are expressed as mean ± SEM of $n = 6–8$ independent experiments per group. *$p < .05$, **$p < .01$ (1-*way* ANOVA).

intracellular pHrodo red intensity at 120 min was enhanced by ~30% in the, 2.5 μM- group, while at 1 μM, 500nM and 50 nM AEA led to a ~40% (yet not statistically significant) increase of the pHrodo intracellular fluorescence (Figure 1B). The strongest effect was exerted by 100 nM AEA, which elicited a significant ($p < .05$) ~100% increase in the amount of HL-60 apoptotic bodies phagocytosed by macrophages at 50 min and 120 min (Figure 1B, D, E), and a significant ($p < .05$) ~100% increase of the area under the curve (A.U.C.) (Figure 1C).

To obtain insights into the mechanisms regulated by AEA to facilitate the uptake of apoptotic cells we next evaluated the expression of efferocytosis receptors on AEA-treated macrophages. Here we observed that the expression of Mer proto-oncogene tyrosine kinase (MerTK) (Figure S1), a protein that has been reported to be involved in efferocytosis,[18] and that of other phagocytosis-associated surface markers such as CD36, CD32 or CD300f (Figure 1G), and scavenger receptors, such as CD163 or CD206 (Figure S1), was unchanged by AEA.

3.2 | CB_2 and GPR18 receptors mediate the AEA-enhanced efferocytosis in MoDMs

Given the ability of AEA to potentiate efferocytosis in MoDMs, we sought to investigate which of the AEA-binding receptors could mediate this activity. Based on the level of expression in MoDMs (Figure S2), CB_2, peroxisome proliferator receptor γ (PPARγ), transient receptor potential cation channel subfamily V member 1 (TRPV1), and GPR18 were chosen as relevant candidates. We incubated MoDMs with 500 nM AM630 (a specific CB_2 antagonist[19]), 1 μM 5′-iodoresinferatoxin (IRTX) (a specific TRPV1 antagonist[20]), 2 μM T0070907 (a specific PPARγ antagonist[21]), or 1 μM O1918 (a specific GPR18 antagonist[22]) (Figure 2A), and evaluated whether any of these antagonists reversed the AEA-enhanced phagocytosis of pHrodo red-labeled apoptotic HL-60. Given that 100 nM represented the lowest significant AEA concentration to exert an effect on efferocytosis this concentration was chosen for these and subsequent experiments. We found that AM630 and O1918 were both able to revert the enhancing effect of AEA on MoDM-mediated efferocytosis (Figure 2B). In particular, these selective antagonists returned the levels of pHrodo red intensity measured at the 150 min interval (Figure 2C), as well as the A.U.C. (Figure 2D), to those measured in Veh-treated cells, whereas antagonism of TRPV1 and PPARγ reversed the effect of AEA to a minor, statistically not significant extent. Macrophages cultured with URB-597 – a selective inhibitor of the main AEA breakdown enzyme, the fatty acid amide hydrolase (FAAH) – to enhance the endogenous production of this eCB exerted no significant effect on efferocytosis (Figure S3B), possibly indicating a low endogenous production of this eCB during the differentiation. We also tested the effect of 2-AG, which engages CB_2 with higher affinity with respect to AEA, but not GPR18: interestingly, 2-AG only elicited a modest and not significant increase in efferocytosis (Figure S3).

To further prove the role of CB_2 and GPR18 in bolstering efferocytosis, we assayed the effect of 100 nM AEA on MoDMs that underwent short interfering RNA (siRNA)-mediated knockdown (KD) for these two receptors (Figure 3A). As expected, siRNA-silenced MoDMs displayed significantly reduced expression of both CB_2 and GPR18 (Figure 3B,C); furthermore, similarly to what we observed in the pharmacological antagonism setup, silencing of these receptors abated the ability of AEA to enhance MoDM-mediated efferocytosis, with CB_2 and GPR18 KD MoDMs displaying pHrodo intensity over 120 min (Figure 3D–F), and overall A.U.C. (Figure 3G) comparable to those of veh-treated cells.

Taken together, these findings strongly suggest that AEA potentiates MoDM-dependent efferocytosis of apoptotic cells by engaging both CB_2 and GPR18.

3.3 | AEA treatment modifies the SPM profiles in MoDMs

Macrophages represent primary effectors of the resolution of inflammation, not only by cleaning up the inflamed site from cellular debris and apoptotic cells but also by actively producing soluble mediators, such as SPMs, that are pivotal orchestrators of the resolution program[3]. Given the observed effect of AEA in amplifying efferocytosis, we next asked whether this eCB might enhance macrophage-dependent resolution by influencing active SPMs production. Using liquid chromatography–tandem mass spectrometry (LC–MS/MS), we profiled lipid mediators derived from DHA, n-3 DPA, EPA, and AA.

AEA treatment of classically-activated MoDMs resulted in a shift in lipid mediator concentrations when compared with cells treated with vehicle alone as demonstrated by a shift in the cluster representing the two groups (Figure 4A). Biosynthetic pathway analysis showed a number of lipid mediators, both pro-inflammatory – e.g., TxB_2 and PGD_2 and PGE_2– and pro-resolving – e.g., several DHA-, n-3 DPA-, EPA- and AA-derived SPMs or their precursors – that accounted for the differences between the Veh- and the AEA-treated group with a VIP >1 (Figure 4B and Table 1). In particular, AEA was effective on the following metabolic

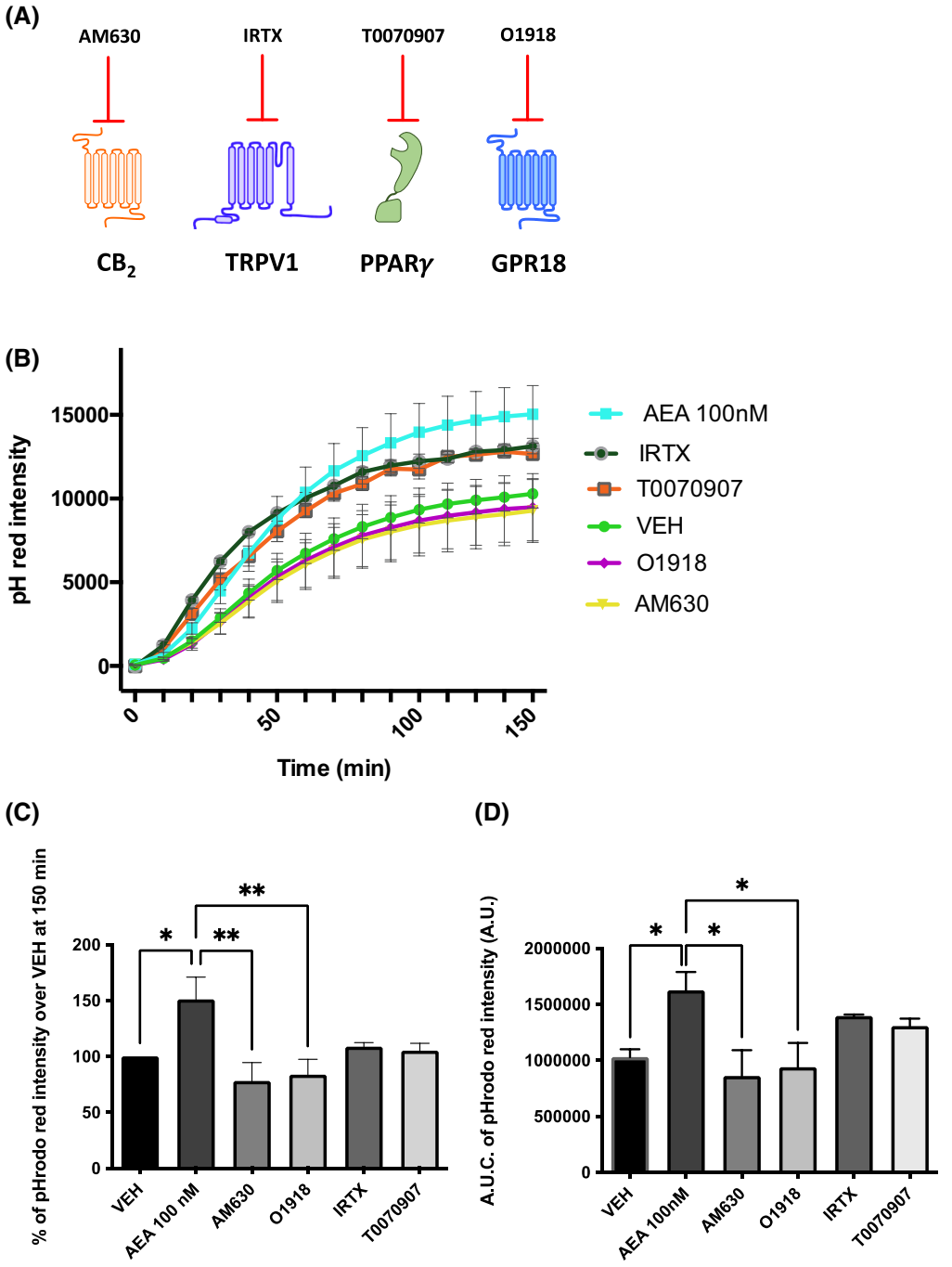

FIGURE 2 Receptors involved in AEA-mediated enhancement of efferocytosis in MoDMs. Selective antagonist are used to specifically target CB_2, TRPV1, PPARγ, and GPR18 (A). Effect of the selective blocking of AEA-binding receptors on efferocytosis of pHrodo red-labeled HL-60 apoptotic cells (B), with detail of their effect at 150 min (C) and on the area under the curve (A.U.C.) (D). All data points are expressed as mean ± SEM of $n = 4–5$ independent experiments per group. *$p < .05$, **$p < .01$ (1-*way* ANOVA).

routes (Figure 4C-F): (i) along the 15-lipoxygenase pathway (ALOX15) it was observed an increase in the levels of RvD1, LXA_4, and LXB_4, and of the n-3 DPA-derived counterpart of RvD2, as well as a concomitant reduction in the levels of RvD3; (ii) along the 12-lipoxygenase pathway (ALOX12) an augmented production of MaR1 and of 4S,14S-diHDHA was demonstrated; (iii) along the cyclooxygenase 2 (COX2)/Cytochrome P450 (CYP450) pathway, AEA-treated macrophages exhibited increased levels of n-3 DPA-derived RvT1, RvT2 and RvT4 and of RvE3; (iv) along the COX pathway AEA enhanced the synthesis of PGD_2 and PGE_2, and concomitantly reduced the synthesis of TXB_2. These results are summarized in Figure 4C, and taken together strongly suggest that AEA has a pleiotropic effect on MoDMs pro-resolving features also by remodulating the SPM production pattern.

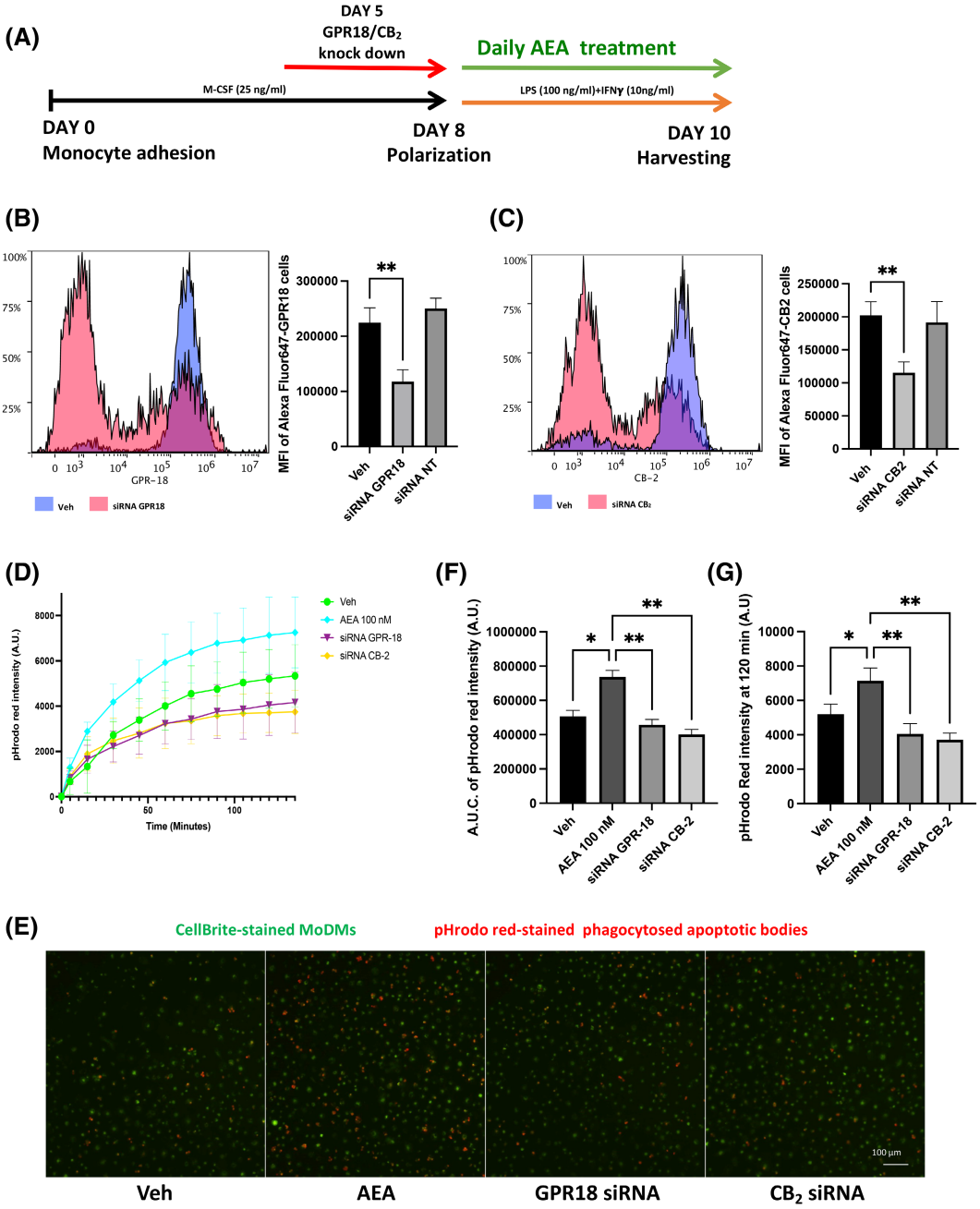

FIGURE 3 Effect of siRNA-mediated knockdown of GR18 and CB_2 on AEA-mediated efferocytosis. Experimental setup used for MoDM differentiation in siRNA-mediated knockdown experiments (A). Expression of GPR18 and CB_2 in MoDM that underwent siRNA knockdown. (B and C). Efferocytosis of pHrodo-labeled apoptotic HL-60 cells in GR18 and CB_2 knockdown MoDMs that underwent AEA treatment (D), with detail of A.U.C. (E) pHrodo intensity at 130 min (F) and phagocytosis of labeled apoptotic cells by means of fluorescence microscopy. (G) Al data points are expressed as mean ± SEM of $n = 4–6$ independent experiments per group. *$p < .05$, **$p < .01$ (1-*way* ANOVA).

3.4 | AEA modulates SPM production in a CB_2-dependent manner

Given the ability of CB_2 and GPR18 to drive AEA-enhanced efferocytosis in MoDMs, we next sought to investigate whether the same receptors are also involved in the AEA-dependent rearrangement of the SPM production pattern in these cells, especially for those lipid species that showed a significant modulation. The Log_2 fold change (FC) vs -Log p-value volcano plot of the analyzed lipids showed a number of SPMs that displayed significant ($p < .05$) modulation upon AEA treatment (Figure 5A). In particular, we observed ~300% upregulation of RvD1 and 22-OH-MaR1 concentrations ($p < .05$; Figure 5B,D), and ~40% increase in MaR2 ($p < .05$) (Figure 5E). We also observed a ~20% increase in RvD6 and RvE2 concentration ($p < .05$) following

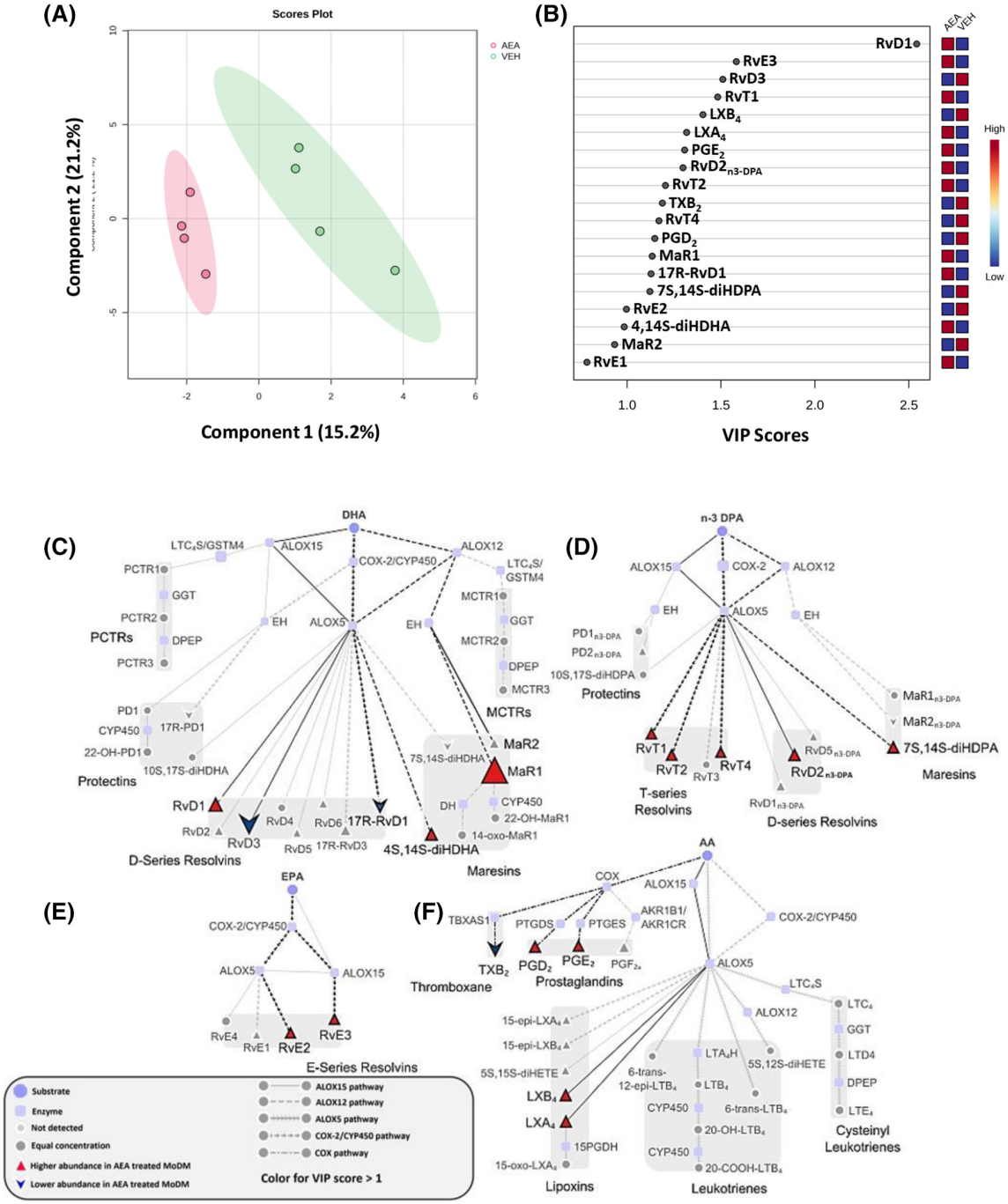

FIGURE 4 Effect of AEA treatment on MoDM-derived production of SPMs. Overall differences between Veh- and AEA-treated MoDMs were evaluated by means of PLS-DA. Scores plot (A); VIP score (B); Pathway analysis highlighting those biosynthetic pathways linked with mediators found to contribute to the separation between vehicle and AEA treatment in the PLS-DA analysis (VIP Scores >1) for mediators from the DHA, (C) n-3 DPA, (D) EPA (E), and AA (F) bioactive metabolomes (C). Results in pathway analysis are expressed as fold-change differences vs concentration in the supernatants of $n = 4–5$ independent experiments per group.

AEA exposure (Figure 5C,G), with respect to Veh-treated MoDMs (Figure 5B). Moreover, among the ~30% of SPMs that were down-regulated by AEA treatment, 22-OH-PD1 was the only one reaching statistical significance ($p < .05$), with a ~300% drop with respect to Veh-treated controls (Figure 5F).

Of note, only CB_2 mediated these effects of AEA: indeed, MoDMs incubated with AM630 showed a significantly lower ($p < .05$) production of RvD1, 22-OH-MaR1, and MaR2 compared to AEA-treated cells, and comparable to controls. Instead, pharmacological antagonism of GPR18 by O1918 only slightly reverted the

TABLE 1 Lipid mediator profile of Veh- and AEA-treated MoDMs.

	Veh	AEA 100nM	
	Average ± SEM	**Average ± SEM**	***p*-value**
DHA-derived mediators, precursors and pathway markers			
RvD1	1.63 ± 0.94	5.13 ± 0.28	0.0162
17R-RvD1	7.51 ± 3.70	6.77 ± 1.94	0.865
RvD2	8.29 ± 2.13	12.29 ± 2.38	0.085
RvD3	9.50 ± 7.66	2.51 ± 2.51	0.4678
17R-RvD3	4.73 ± 1.32	5.29 ± 1.45	0.391
RvD4	47.83 ± 8.88	45.93 ± 6.18	0.8985
RvD5	91.09 ± 21.57	99.89 ± 30.82	0.4452
RvD6	174.76 ± 52.40	212.28 ± 59.24	0.0382
22-OH-PD1	9.58 ± 3.27	3.52 ± 1.55	0.0395
17R-PD1	9.45 ± 2.12	8.07 ± 2.03	0.3152
MaR1	78.75 ± 6.57	81.84 ± 4.48	0.9605
MaR2	176.40 ± 9.97	333.82 ± 56.54	0.0126
22-OH-MaR1	142.57 ± 53.59	425.06 ± 113.05	0.034
4,14s-diHDHA	65.56 ± 38.70	130.40 ± 75.36	0.1958
4HDHA	1333.29 ± 632.92	1216.42 ± 464.04	0.5874
7HDHA	753.05 ± 212.22	777.90 ± 216.22	0.226
13HDHA	733.65 ± 322.84	667.85 ± 247.19	0.5019
14HDHA	486.45 ± 164.63	464.79 ± 143.50	0.5794
17HDHA	791.61 ± 361.28	704.83 ± 260.98	0.4642
10S,17S-diHDHA	348.41 ± 86.36	433.75 ± 134.17	0.1964
7S,14S-diHDHA	51.84 ± 18.11	62.29 ± 21.27	0.075
DHA	7361.37 ± 2418.71	7466.39 ± 2540.08	0.8521
n-3 DPA-derived mediators, precursors and pathway markers			
$RvD1_{n\text{-}3\ DPA}$	7.50 ± 1.97	12.20 ± 3.27	0.0686
$RvD2_{n\text{-}3DPA}$	1.57 ± 0.13	2.72 ± 1.46	0.484
$RvD5_{n\text{-}3DPA}$	125.70 ± 26.18	142.33 ± 33.01	0.1128
RvT1	9.21 ± 3.50	12.08 ± 1.47	0.3316
RvT2	3.30 ± 1.33	4.75 ± 1.06	0.2591
RvT4	251.83 ± 50.60	262.48 ± 54.89	0.5576
$PD1_{n\text{-}3\ DPA}$	18.69 ± 6.52	18.97 ± 7.84	0.9269
$PD2_{n\text{-}3\ DPA}$	16.41 ± 9.58	17.86 ± 10.32	0.3087
$22\text{-}OH\text{-}PD1_{n\text{-}3\ DPA}$	2.94 ± 0.38	3.61 ± 1.96	0.7275
$MaR2_{n\text{-}3\ DPA}$	1609.46 ± 271.60	1514.90 ± 162.36	0.5617
7-HDPA	256.13 ± 152.40	261.88 ± 150.51	0.7334
13-HDPA	69.45 ± 21.85	67.87 ± 17.28	0.7608
14-HDPA	266.95 ± 158.46	285.29 ± 172.03	0.3503
17-HDPA	952.62 ± 316.48	897.06 ± 236.11	0.5611
7S,14S-diHDPA	18.24 ± 18.24	28.75 ± 28.75	0.391
DPA	3125.49 ± 961.04	3191.78 ± 1046.54	0.8268
EPA-derived mediators, precursors and pathway markers			
RvE1	0.27 ± 0.16	0.32 ± 0.20	0.4027
RvE2	402.73 ± 87.81	469.10 ± 99.21	0.0327

TABLE 1 (Continued)

	Veh	AEA 100nM	
	Average ± SEM	**Average ± SEM**	***p*-value**
RvE3	137.25 ± 9.73	170.45 ± 35.49	0.3281
5-HEPE	1319.14 ± 450.14	1400.04 ± 474.98	0.1385
11-HEPE	717.31 ± 330.95	650.53 ± 243.57	0.5171
12-HEPE	626.31 ± 238.99	547.70 ± 171.07	0.3901
15-HEPE	403.05 ± 160.39	472.71 ± 187.75	0.1042
18-HEPE	3122.50 ± 923.28	3716.97 ± 1210.54	0.1374
EPA	1772.35 ± 647.27	1829.43 ± 659.55	0.1414
AA-derived metabolome			
LXA_4	88.65 ± 24.13	144.15 ± 35.24	0.166
LXB_4	152.83 ± 63.47	238.40 ± 30.71	0.2187
15-epi-LXA_4	115.59 ± 11.91	145.35 ± 32.92	0.3422
15-epi-LXB_4	1434.03 ± 327.96	1672.66 ± 605.62	0.4636
13,14-dehydro-15-oxo-LXA_4	20.93 ± 13.43	8.78 ± 5.26	0.3148
15-oxo-LXA_4	2.08 ± 0.26	3.11 ± 0.90	0.3132
5-HETE	2684.87 ± 1101.31	2565.40 ± 886.41	0.7093
12-HETE	2192.64 ± 744.63	2120.94 ± 633.89	0.651
15-HETE	4789.55 ± 1935.81	4891.53 ± 1759.53	0.7556
20-HETE	2754.40 ± 673.45	2667.56 ± 655.61	0.6917
5S,15S-diHETE	524.09 ± 101.01	668.95 ± 213.38	0.3247
LTB_4	ND	ND	
20-OH-LTB_4	0.94 ± 0.64	0.42 ± 0.27	0.2498
20-COOH-LTB_4	3.00 ± 1.84	4.23 ± 2.46	0.3494
PGE_2	63.61 ± 15.07	81.98 ± 3.66	0.3146
PGD_2	22.45 ± 7.88	33.78 ± 5.48	0.1515
$PGF_{2\alpha}$	70.73 ± 15.66	156.76 ± 67.01	0.2727
TxB_2	751.05 ± 123.28	568.46 ± 121.16	0.0716
AA	13017.24 ± 3879.61	13793.24 ± 4354.71	0.2673

effects of AEA on RvD1, 22-OH-MaR1, and MaR2 production (Figure 5B,D,E) and did not reach statistical significance.

Interestingly, the AEA-dependent modulation of RvD6, 22-OH-PD1, and RvE2 could not be reversed by either AM630 or O1918 (Figure 5C,F,G), suggesting a more complex mechanism behind the ability of AEA to modulate SPM production. Taken together, these data suggest that CB_2 might be a crucial orchestrator of the effects of AEA on the SPM biosynthetic properties of MoDMs.

3.5 | AEA modulation on the expression of SPM biosynthetic and breakdown enzymes

Next, we sought to ascertain whether the observed ability of AEA to act on SPM production in MoDMs was also accompanied by a concomitant modulation of the gene and protein expression of the main enzymes involved in the biosynthesis (i.e., ALOX5, ALOX12, and ALOX15) or inactivation (i.e., 15-prostaglandin dehydrogenase (15-PGDH)) of SPM, and whether CB_2 was engaged also in these effects. Indeed, AEA-treated MoDMs displayed a significant ($p < .05$) ~300% increase in the expression of *ALOX5* gene and a concomitant ~60% downregulation of the *15-PGDH* gene (Figure 6A). This effect was reversed by the concomitant incubation with AM630. Instead, AEA failed to elicit any significant effect on the gene expression of *ALOX12* and *ALOX15*.

Then, we sought to investigate whether the observed effect of AEA on ALOX5 and *15-PGDH* gene expression was reflected by a concomitant upregulation of the corresponding protein products. Thus, by means of polychromatic flow cytometry we analyzed the protein expression of the same SPM metabolic enzymes. As shown in

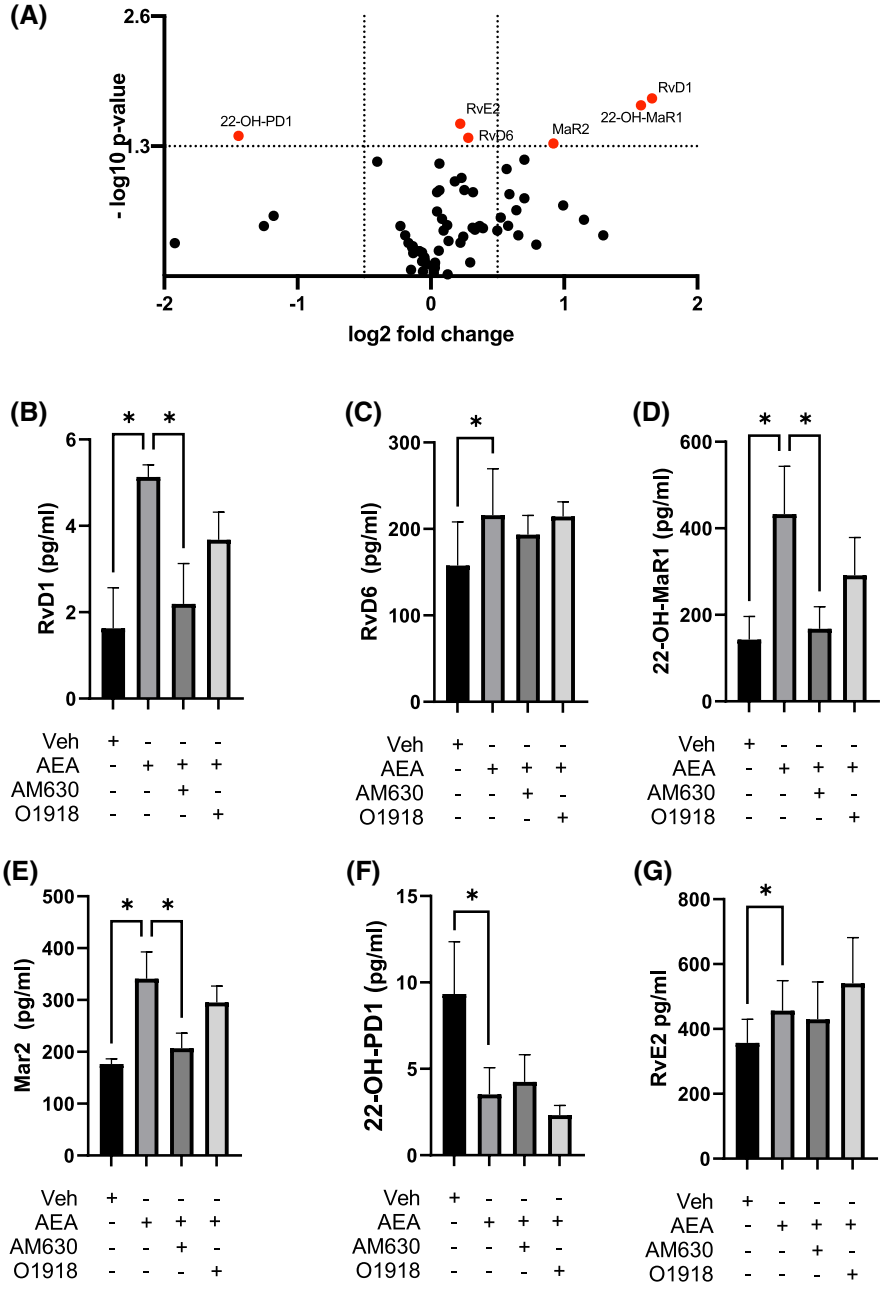

FIGURE 5 Role of CB_2 and GPR18 on lipid mediators that resulted significantly modulated following AEA treatment. Volcano plot of −Log *p* value (Student's *t* test of AEA vs Veh) vs Log2 fold change of the SPM levels produced by MoDMs (A), showing the lipid species that display significant ($p < .05$, or −Log *p* value >1.3) modulation. Each data point represents the mean of 4–5 independent experiments. Effect of CB_2 and GPR18 pharmacological antagonism on the production of RvD1, RvD6, 22-OH-MaR1, MaR2, 22-OH-PD1, and RvE2 (B-G) in Veh and AEA-treated MoDMs. All data are showed as mean ± SEM of $n = 4–5$ independent experiments per group. *$p < .05$, (1-*way* ANOVA).

Figure 6C, intracellular expression of ALOX5 displayed a ~30% upregulation, which however did not reach statistical significance, whereas 15-PGDH expression remained unchanged. The antagonism of CB_2 by AM630 did not exert any significant effect on the expression of both targets. The gating strategy for the polychromatic flow cytometry experiments is summarized in Figure 6B.

Furthermore, of the SPM receptors for which gene expression was analyzed, only *GPR32* and *ChemR23* genes were downregulated upon AEA treatment, an effect that was reversed by AM630; yet, under the same conditions, AEA did not affect the corresponding protein products (Figure S4A,B).

4 | DISCUSSION

Endocannabinoids – AEA in particular – are involved in several immune processes that control the course and outcome of the inflammatory event suggesting their role, alongside SPMs, in tissue homeostasis and resolution of inflammation. Macrophages represent ideal target for this concerted action, by virtue of their critical role in coordinating immune events and their aftermath.[5] On the other hand, despite a number of papers documenting the ability of AEA to regulate the immunomodulatory properties of macrophages,[7,16,17] the role of this eCB in activating resolution mechanisms has not

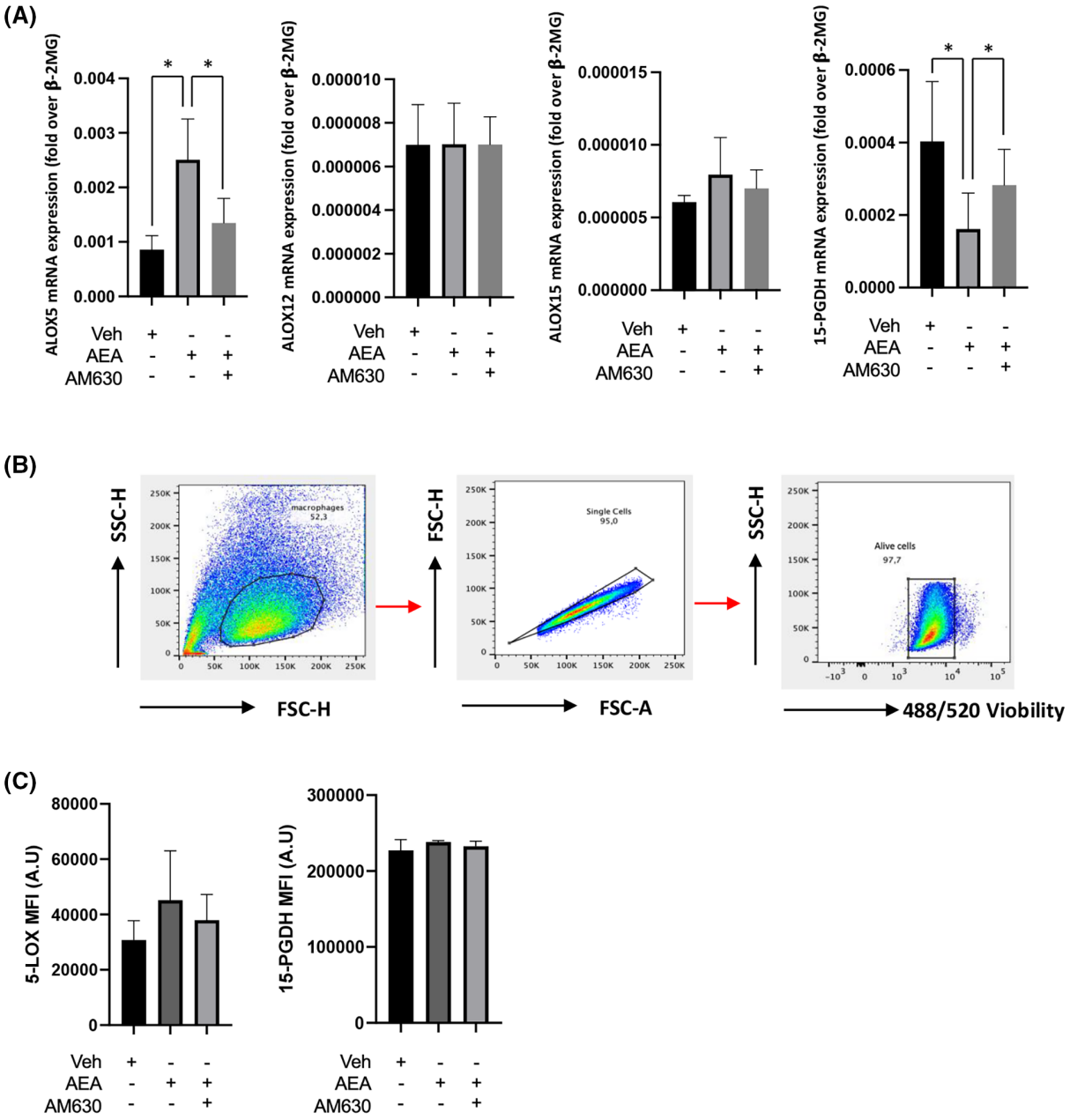

FIGURE 6 Effect of AEA on the expression of the main SPM biosynthetic and breakdown enzymes. mRNA expression by means of quantitative RT-PCR of 5-, 12- and ALOX15, and of 15-PGDH in MoDMs (A). Data are showed as mean ± SEM of $n = 7–8$ independent experiments per group. *$p < .05$ (1-*way* ANOVA); Protein expression of ALOX5 and 15-PGDH by means of polychromatic flow cytometry, with gating strategy (B) and mean fluorescence intensity levels (C), Data are showed as mean ± SEM of $n = 7–8$ independent experiments per group.

been yet investigated in detail. Although the eCB system has been previously postulated to be an intermediary in the pro-resolving effects of certain PUFA-based dietary interventions,[23] our study is the first to report a direct role of AEA in adjuvating SPMs during the resolution program.

In the present study, we observed that AEA in the nanomolar range (100 nM) induces efferocytosis in human primary MoDMs by engaging both CB_2 and GPR18. Macrophage-mediated efferocytosis is a central process that facilitates the resolution of inflammation by removing tissue debris and dead cells resulting from acute inflammation, preventing secondary necrosis and propagation of the inflammatory response. Moreover, efferocytic macrophages upregulate the formation of further SPMs.[3] Anandamide might well improve in vivo resolution by enhancing the production of pro-resolving lipids through this mechanism.

Although to date the mechanism of intracellular trafficking that leads to the release of AEA is still debated,[24] pioneering studies showed that primary mouse macrophages and RAW 264.7 cell lines can produce AEA, upon LPS stimulation, in the picomolar range,[25–27] which might explain why URB-597 could not mimic the effects of the 100 nM AEA treatment and drive sufficient accumulation of this endocannabinoid to exert any efficacy on efferocytosis. Yet again, the dose we utilized in the present work might be reached in vivo either by longer times or through the production from other cognate cells. Furthermore, the observed GPR18 dependency of AEA-potentiating effect not only reinforces the role of this receptor in proper resolution but also strengthens the idea that its ligand promiscuity for RvD2 and AEA[11] might play an important part in the cross-talk between SPMs and eCBs during the control of the inflammatory outcome. In particular, GPR18 and CB_2 might act synergistically, as suggested by the fact that their individual inactivation reverts AEA-mediated efferocytosis, while administration of 2-AG – which acts as an agonist to CB_2 but not to GPR18 – only slightly enhances efferocytosis. To our knowledge, a single study to date reported an enhancing effect of CB_2 on macrophagic efferocytosis,[12] however, not only this study was carried out on peritoneal macrophages and RAW264.7 cells, but also made use of potently selective compounds (e.g., JWH-133 and HU-308) which display an affinity for this receptor that is far greater than that of either AEA or 2-AG.[28]

Also of note, not only GPR18 was primarily identified as the receptor of *N*-arachidonoylglycine (NAGly), but it is also able to dimerize with CB_2,[29] suggesting that resolution might be achieved by the concerted action of SPMs alongside *N*-acetylethanolamines (NAEs).

Curiously, we found that the antagonism of neither TRPV1 nor PPARγ was able to revert AEA-enhanced efferocytosis in MoDMs, regardless of their ability to bind AEA[30,31]: while to our knowledge no evidence is available for an involvement of TRPV1 in mediating the pro-efferocytosis activities of phagocytes, PPARγ mediates phagocytosis of apoptotic cells in alveolar macrophages of bleomycin-induced fibrosis mouse models[32] and in peritoneal macrophages of mice that were challenged with zymosan.[33] Since macrophages that surveil different tissues and environments display functional and immunophenotypic heterogeneity,[34] a difference in the quality of the inflammatory milieu or in the macrophage receptor repertoire between these paradigms and ours might be responsible for the lack of involvement in PPARγ in our experiments. We did not observe any significant differences in the expression of phagocytosis or scavenger receptors – which are associated with pro-resolving phenotypes in macrophages[35,36] – nor of pro-inflammatory M1-like markers such as CD80 and CD54 (data not shown) following AEA treatment. This conflicts with a number of studies that have previously reported a role of CB_2 signaling in M2-like polarization.[37–39] It should be noted, however, that not only these studies were mostly conducted using CB_2 selective agonists but also that the authors that reported M2-like polarizing/M1-like antagonizing properties of AEA were conducted in microglia, as reviewed in[40] and used this eCB in the micromolar ranges (up to 10 μM), as opposed to the nanomolar concentrations that we see being effective in the present work. Quite intriguingly, the effect of AEA on efferocytosis is independent of MerTK, which raises the compelling possibility that concomitant activation of CB_2 and GPR18 might trigger this mechanism through other pathways: since MerTK has often been involved in immune suppression and tumor progression,[41,42] AEA (or CB_2/GPR18 combined signaling) might promote clearance processes without the concomitant activation of signals that might help malignant lesions to evade immune surveillance and T cell cytotoxic response.

We also observed a substantial rearrangement in the biosynthetic pattern of SPMs, with ~70% of the measured lipids undergoing upregulation, despite a lack of effect of AEA treatment on the protein expression of none of the main SPM biosynthetic enzymes (i.e., 5-, 12- and ALOX15). Furthermore, the fact that a number of SPMs are significantly upregulated (i.e., RvD1, RvD6, 22-OH-MaR1, MaR2, and RvE2) following treatment of the cells with AEA suggests that this eCB might contribute to macrophage-mediate resolution by enhancing the biosynthesis of important pro-resolving lipids. Of interest, CB_2 seemed to be the major player in the enhancement of SPM biosynthesis elicited by AEA treatment, whereas GPR18 did not seem to be involved. On the other hand, for some SPMs (i.e., RvD6, 22-OH-PD1, and RvE2), neither CB_2 nor GPR18 seemed to be involved, either suggesting the activity of other receptors or the presence of entirely different mechanisms. Interestingly, NAEs have been reported to directly induce phospholipase A_2 (PLA_2) activity by physically interacting with the cell membrane[43]; even though in this paper, this effect was mostly observed in unsaturated NAEs, this demonstrates that these molecules can act on the intracellular availability of *sn*-2 bound fatty acids in phospholipids in a receptor-independent manner, which might result in changes in the production of PUFA-derived autacoids. LPS-based polarization failed to induce the production of relevant amounts of LTB_4 – nor could AEA affect its biosynthesis: this lipid is instead usually produced by activated polymorphonuclear cells (PMN) in order to target macrophages, which express its receptor targets BLT1 and BLT2[44,45]. LTB_4 might yet be produced in small amounts by MoDMs, and promptly converted into its downstream hydroxylated and carboxylated metabolites, as suggested

by the low levels of 20-OH- and 20-COOH-LTB_4 that we detected in our experiments (as shown in Table 1). Lack of effect AEA on the protein expression of 15-PGDH by AEA, alongside the evidence that no SPM oxo-derivative was found as significantly increased in our experiments, suggests that the rearrangement of the biosynthetic tone of SPMs does not depend on the inactivating action of this enzyme. Similarly, ALOX5 mRNA, but not its 5-LOX protein product, underwent upregulation: this might be explained by an increased activity of the enzyme elicited by AEA. A recent work has showed that the phytocannabinoid cannabidiol (CBD) can elicit allosteric modulation of 15- and 5-LOX by binding to their interdomain cleft,[46,47] thus influencing the positioning of the PUFA substrate. AEA might act in a similar way and promote the biosynthesis of SPMs.

Taken together, findings made in our study highlight a role for AEA in facilitating the resolution of inflammation by regulating macrophage responses, upregulating the production of SPM and the ability of these cells to clear apoptotic cells and tissue debris in a CB_2- and GPR18-dependent manner. These findings support the notion that different lipid species participate in concert to achieve immune modulation, in a wider network, which might well include other lipid congeners that are involved in immune control.

4.1 | Significance

Resolution of inflammation is crucial in controlling the outcome of immune events and in avoiding their transition to chronic processes. Unsurprisingly, impaired resolution has been observed in a number of inflammatory diseases. Accumulated evidence during the last two decades suggests that tissue homeostasis might be a rather complex process, where the action of SPMs in self-resolving contexts might be very likely adjuvated by other lipids that control immune balance as a whole. Understanding how different lipid congeners – especially those that have consistently been involved in immunomodulation such as eCBs – participate alongside SPMs in resolution is crucial to fully characterize this process in its entirety and design possible enhancing therapies that exploit the synergy between its different players. Our data show that the main eCB AEA acts on crucial resolution-related aspects, both enhancing macrophage-mediated efferocytosis and modulating the production of pro-resolving lipids in human primary macrophages. Interestingly, this action not only depends on the canonical eCB receptor CB_2 but also on GPR18, which is known to bind both DHA-derived RvD2 and AEA. Nevertheless, despite its therapeutic potential, an effect of eCBs on proper pro-resolving properties has never been investigated in detail. Our study fills this gap and strongly supports the possibility that tissue homeostasis might result from concerted action of a larger cohort of lipids, other than SPMs. The importance of the cannabinoid/endocannabinoid signaling in this landscape is reinforced by the well-known fact that also phytocannabinoids such as Δ9-tetrahydrocannabinol and cannabidiol exert anti-inflammatory actions – especially in light of the fact that plant-derived cannabinoids are thought to engage other receptors, besides CB_1 and CB_2 and, as recently demonstrated, to adjuvate pro-resolving processes.[46]

AUTHOR CONTRIBUTIONS

A. Leuti, J. Dalli, and M. Maccarrone designed the research; A. Leuti, M. Fava, N. Pellegrini, L. Scipioni, E.A. Gomez, and G. Forte conducted research and analyzed data; S. Oddi, J. Dalli, and M. Maccarrone provided reagents and analytic tools. A. Leuti and M. Fava drafted the paper; S. Oddi, J. Dalli, and M. Maccarrone revised the paper.

ACKNOWLEDGMENTS

Funded by the European Union - Next Generation EU - NRRP M6C2 - Investment 2.1 Enhancement and strenghtening of biomedical research in the NHS, prot. N. PNRR-MAD-2022-12376730 to MM and SO.

DISCLOSURES

The authors have no conflicts of interest to disclose with regard to the present work.

DATA AVAILABILITY STATEMENT

None of the data supporting the findings of this study were derived from public repositories or databases. The mass spectrometry data are entirely available on this paper in Table 1.

ORCID

Alessandro Leuti https://orcid.org/0000-0002-5982-0682
Marina Fava https://orcid.org/0000-0003-4593-7799
Giulia Forte https://orcid.org/0009-0004-4592-6840
Niccolò Pellegrini https://orcid.org/0000-0003-4539-7614
Sergio Oddi https://orcid.org/0000-0002-6217-698X
Lucia Scipioni https://orcid.org/0000-0003-4764-8296
Esteban A. Gomez https://orcid.org/0000-0001-8028-416X
Jesmond Dalli https://orcid.org/0000-0001-6328-3640
Mauro Maccarrone https://orcid.org/0000-0002-3990-2963

REFERENCES

1. Serhan CN, Levy BD. Resolvins in inflammation: emergence of the pro-resolving superfamily of mediators. *J Clin Invest*. 2018;128:2657-2669.
2. Serhan CN. Discovery of specialized pro-resolving mediators marks the dawn of resolution physiology and pharmacology. *Mol Asp Med*. 2017;58:1-11.
3. Dalli J, Serhan CN. Pro-resolving mediators in regulating and conferring macrophage function. *Front Immunol*. 2017;8: 1400.
4. Chiurchiù V, Leuti A, Dalli J, et al. Proresolving lipid mediators resolvin D1, resolvin D2, and maresin 1 are critical in modulating T cell responses. *Sci Transl Med*. 2016;8:353ra111.
5. Leuti A, Fazio D, Fava M, Piccoli A, Oddi S, Maccarrone M. Bioactive lipids, inflammation and chronic diseases. *Adv Drug Deliv Rev*. 2020;159:133-169.
6. Chiurchiù V, Leuti A, Maccarrone M. Bioactive lipids and chronic inflammation: managing the fire within. *Front Immunol*. 2018;9:38.
7. Chiurchiù V, Scipioni L, Arosio B, Mari D, Oddi S, Maccarrone M. Anti-inflammatory effects of fatty acid amide hydrolase inhibition in monocytes/macrophages from Alzheimer's disease patients. *Biomolecules*. 2021;11:502.
8. Cencioni MT, Chiurchiù V, Catanzaro G, et al. Anandamide suppresses proliferation and cytokine release from primary human T-lymphocytes mainly via CB2 receptors. *PLoS One*. 2010;5:e8688.
9. Leuti A, Fava M, Pellegrini N, Maccarrone M. Role of specialized pro-resolving mediators in neuropathic pain. *Front Pharmacol*. 2021;12:717993.
10. Chiang N, Dalli J, Colas RA, Serhan CN. Identification of resolvin D2 receptor mediating resolution of infections and organ protection. *J Exp Med*. 2015;212:1203-1217.
11. Console-Bram L, Brailoiu E, Brailoiu GC, Sharir H, Abood ME. Activation of GPR18 by cannabinoid compounds: a tale of biased agonism. *Br J Pharmacol*. 2014;171:3908-3917.
12. Jiang L, Chen Y, Huang X, et al. Selective activation of CB2 receptor improves efferocytosis in cultured macrophages. *Life Sci*. 2016;161:10-18.
13. Flak MB, Koenis DS, Sobrino A, et al. GPR101 mediates the pro-resolving actions of $RvD5_{n\text{-}3\ DPA}$ in arthritis and infections. *J Clin Invest*. 2020;130:359-373.
14. Koenis DS, Beegun I, Jouvene CC, et al. Disrupted resolution mechanisms favor altered phagocyte responses in COVID-19. *Circ Res*. 2021;129:e54-e71.
15. Xia J, Psychogios N, Young N, Wishart DS. MetaboAnalyst: a web server for metabolomic data analysis and interpretation. *Nucleic Acids Res*. 2009;37:W652-W660.
16. Chiurchiù V, Leuti A, Cencioni MT, et al. Modulation of monocytes by bioactive lipid anandamide in multiple sclerosis involves distinct toll-like receptors. *Pharmacol Res*. 2016;113:313-319.
17. Cabral GA, Ferreira GA, Jamerson MJ. Endocannabinoids and the immune system in health and disease. In: Pertwee RG, ed. *Endocannabinoids*. Springer International Publishing; 2015:185-211.
18. Rymut N, Heinz J, Sadhu S, et al. Resolvin D1 promotes efferocytosis in aging by limiting senescent cell-induced MerTK cleavage. *FASEB J*. 2020;34:597-609.
19. Ross RA, Brockie HC, Stevenson LA, et al. Agonist-inverse agonist characterization at CB1 and CB2 cannabinoid receptors of L759633, L759656, and AM630. *Br J Pharmacol*. 1999;126:665-672.
20. De Petrocellis L, Schiano Moriello A, Imperatore R, Cristino L, Starowicz K, Di Marzo V. A re-evaluation of 9-HODE activity at TRPV1 channels in comparison with anandamide: enantioselectivity and effects at other TRP channels and in sensory neurons. *Br J Pharmacol*. 2012;167:1643-1651.
21. Lee G, Elwood F, McNally J, et al. T0070907, a selective ligand for peroxisome proliferator-activated receptor gamma, functions as an antagonist of biochemical and cellular activities. *J Biol Chem*. 2002;277:19649-19657.
22. Morales P, Lago-Fernandez A, Hurst DP, et al. Therapeutic exploitation of GPR18: beyond the cannabinoids? *J Med Chem*. 2020;63:14216-14227.
23. Komarnytsky S, Rathinasabapathy T, Wagner C, et al. Endocannabinoid system and its regulation by polyunsaturated fatty acids and full Spectrum hemp oils. *Int J Mol Sci*. 2021;22:5479.
24. Maccarrone M, Di Marzo V, Gertsch J, et al. Goods and Bads of the endocannabinoid system as a therapeutic target: lessons Learned after 30 years. *Pharmacol Rev*. 2023;75:885-958.
25. Liu J, Batkai S, Pacher P, et al. Lipopolysaccharide induces anandamide synthesis in macrophages via CD14/MAPK/phosphoinositide 3-kinase/NF-kappaB independently of platelet-activating factor. *J Biol Chem*. 2003;278:45034-45039.
26. Liu J, Wang L, Harvey-White J, et al. Multiple pathways involved in the biosynthesis of anandamide. *Neuropharmacology*. 2008;54:1-7.
27. Jiang L, Pu J, Han Z, Hu L, He B. Role of activated endocannabinoid system in regulation of cellular cholesterol metabolism in macrophages. *Cardiovasc Res*. 2009;81:805-813.
28. Steffens S, Pacher P. Targeting cannabinoid receptor CB2 in cardiovascular disorders: promises and controversies. *Br J Pharmacol*. 2012;167:313-323.
29. Reyes-Resina I, Navarro G, Aguinaga D, et al. Molecular and functional interaction between GPR18 and cannabinoid CB2 G-protein-coupled receptors. Relevance in neurodegenerative diseases. *Biochem Pharmacol*. 2018;157:169-179.
30. O'Sullivan SE. An update on PPAR activation by cannabinoids. *Br J Pharmacol*. 2016;173:1899-1910.
31. Muller C, Lynch DL, Hurst DP, Reggio PH. A closer look at anandamide interaction with TRPV1. *Front Mol Biosci*. 2020;7:144.
32. Yoon Y-S, Kim S-Y, Kim M-J, Lim J-H, Cho M-S, Kang JL. PPARγ activation following apoptotic cell instillation promotes resolution of lung inflammation and fibrosis via regulation of efferocytosis and proresolving cytokines. *Mucosal Immunol*. 2015;8:1031-1046.
33. Fernandez-Boyanapalli R, Frasch SC, Riches DWH, Vandivier RW, Henson PM, Bratton DL. PPARγ activation normalizes resolution of acute sterile inflammation in murine chronic granulomatous disease. *Blood*. 2010;116:4512-4522.
34. Gordon S, Plüddemann A. Tissue macrophages: heterogeneity and functions. *BMC Biol*. 2017;15:53.
35. Werz O, Gerstmeier J, Libreros S, et al. Human macrophages differentially produce specific resolvin or leukotriene signals that depend on bacterial pathogenicity. *Nat Commun*. 2018;9:59.
36. Elliott MR, Koster KM, Murphy PS. Efferocytosis signaling in the regulation of macrophage inflammatory responses. *J Immunol*. 2017;198:1387-1394.
37. Braun M, Khan ZT, Khan MB, et al. Selective activation of cannabinoid receptor-2 reduces neuroinflammation after

traumatic brain injury via alternative macrophage polarization. *Brain Behav Immun*. 2018;68:224-237.
38. Du Y, Ren P, Wang Q, et al. Cannabinoid 2 receptor attenuates inflammation during skin wound healing by inhibiting M1 macrophages rather than activating M2 macrophages. *J Inflamm*. 2018;15:25.
39. Tomar S, Zumbrun E, Nagarkatti M, Nagarkatti PS. Protective role of cannabinoid receptor 2 activation in galactosamine/lipopolysaccharide-induced acute liver failure through regulation of macrophage polarization and microRNAs. *J Pharmacol Exp Ther*. 2015;353:369-379.
40. Tanaka M, Sackett S, Zhang Y. Endocannabinoid modulation of microglial phenotypes in neuropathology. *Front Neurol*. 2020;11: 87.
41. Lin J, Xu A, Jin J, et al. MerTK-mediated efferocytosis promotes immune tolerance and tumor progression in osteosarcoma through enhancing M2 polarization and PD-L1 expression. *Onco Targets Ther*. 2022;11:2024941.
42. Zhou Y, Fei M, Zhang G, et al. Blockade of the phagocytic receptor MerTK on tumor-associated macrophages enhances P2X7R-dependent STING activation by tumor-derived cGAMP. *Immunity*. 2020;52:357-373.e9.
43. Zolese G, Wozniak M, Mariani P, Saturni L, Bertoli E, Ambrosini A. Different modulation of phospholipase A2 activity by saturated and monounsaturated N-acylethanolamines. *J Lipid Res*. 2003;44:742-753.
44. Zhang Y, Olson RM, Brown CR. Macrophage LTB4 drives efficient phagocytosis of borrelia burgdorferi via BLT1 or BLT2. *J Lipid Res*. 2017;58:494-503.
45. Li P, Oh DY, Bandyopadhyay G, et al. LTB4 promotes insulin resistance in obese mice by acting on macrophages, hepatocytes and myocytes. *Nat Med*. 2015;21:239-247.
46. Peltner LK, Gluthmann L, Börner F, et al. Cannabidiol acts as molecular switch in innate immune cells to promote the biosynthesis of inflammation-resolving lipid mediators. *Cell Chem Biol*. 2023;30:1508-1524.e7.
47. Leuti A, Fava M, Maccarrone M. A game of networks: do different lipids interact to orchestrate inflammatory homeostasis? *Cell Chem Biol*. 2023;30:1499-1501.

SUPPORTING INFORMATION

Additional supporting information can be found online in the Supporting Information section at the end of this article.

How to cite this article: Leuti A, Fava M, Forte G, et al. The endocannabinoid anandamide activates pro-resolving pathways in human primary macrophages by engaging both CB_2 and GPR18 receptors. *The FASEB Journal*. 2024;38:e23675. doi:10.1096/fj.202301325R